

## The Construction and Operation of a Nine Inch Cyclotron

Timothy W. Koeth

A cyclotron for producing one million volt protons has recently been found useful in low energy nuclear physics research. In designing this small cyclotron the first practical goal set was to use a moderately sized, nine-inch electromagnet to test operational feasibility. Upon successful beam detection, a twelve-inch magnet upgrade will enable the goal of one

million volt protons to be achieved. Construction details of this nine inch machine are given. Several noteworthy and unique features of this cyclotron will be discussed. It has been found that this cyclotron can easily and reliably produce five hundred-thousand volt protons.

I. MAGNET CONSIDERATIONS. The key most element of any cyclotron is the uniform magnetic field which is used to bend the accelerated ions on their outward spiraling course to the target or collector. The most accessible magnet was a Varian V-3400 NMR magnet. It is of the typical H-frame design. Slight modifications were made to utilize the V-3400. Mounting the magnet sideways on a table created a horizontal gap at a reasonable work height. New pole tips were machined from 1020 rolled steel into cylinders, maximizing the diameter. The poles are nine inches in diameter and create a gap of 2.1875 inches. The maximum field obtainable from this geometry is 1.2 Tesla. The operating field value was determined by the oscillator. For reasons that will be discussed later the operating frequency is  $13.56 \pm 0.03$  MHz. Using the cyclotron frequency relationship:

$$f = qB/2\pi m$$

a magnetic field of 0.889 Tesla was determined to be the operating field value. This was a welcome operating value, as the magnet need only be run at 70 percent of its maximum values, reducing the chance of coil failure by pressing the tolerances.

The magnet weighs 1780 pounds, it requires 40 volts at 168 amps, 7Kilowatts, to produce the maximum field of 1.2 Tesla. Only 28 volts at 114 amps, 3.2 kW, is required at the operating value of 0.889 Tesla. Water cooling is used to remove the heat generated by the coils, the inlet pressure is approximately 38 PSI and flow rate is no less than 4 GPM. The pressure is controlled with an inline pressure regulator and the flow

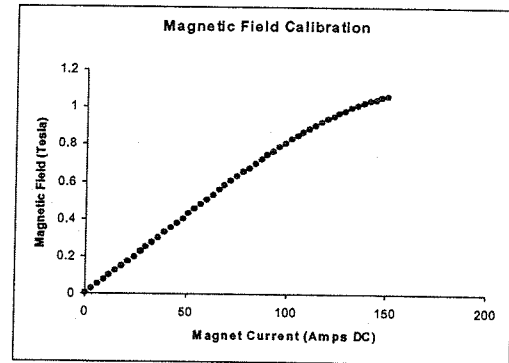


Fig.1 Magnetic Field Calibration of V-3400

rate is monitored with an impeller driven magnetic pick-up digital flow meter.

Power is obtained from a Sorenson DCR-40-250A DC 10kW power supply. It has input requirements of 208Vrms 3-Phase at 60 Amps and is only forced air cooled. The DCR-40-250A has the ability to be "programmed" remotely, either by an external variable voltage or current source or a variable resistance. This option ultimately allowed the magnetic field to be computer controlled by interfacing a Fluke 4210 BCD programmable DC voltage source. The method of controlling the 4210 is via the IEEE-488 standard, also know as GPIB. The output range of the 4210 is 0 to 10.000 volts in 1 millivolt steps, while the input programming voltage required by the DCR-40-250A is 0 to approximately 8.00 Volts at maximum output. Since the maximum magnetic field of 1.2 Tesla requires a maximum programming voltage of 6.00 volts into the DCR-40-250A, theoretically the magnetic field could be adjusted to one part

in six thousand or 2 gauss. Practically though, the field control was less than the theoretical as variations in cooling water temperature would change the resistance of the coils. The DC power system being voltage regulated then caused changes in the magnet current and of course the magnetic field.

A magnetic field calibration to determine the field as a function of applied current was done in order to simplify the data collection. A precision shunt of 1.00 mΩ was inserted into the magnet DC power lead, a 5 digit Keithly DVM measured the voltage drop across the shunt. A Bell 620 Hall Effect Gaussmeter measured the field, while another Keithly DVM measured the 620's recorder output. The Hall Effect probe was located centered, flat against the surface of the bottom pole piece. An HP85 HP-IB based computer was employed to slowly ramp the magnetic field while, while reading the values of the two meters. The data was then recorded to an IBM PC disk via an RS232 link. Fig.1 shows the calibration plot.

A radial measurement of the magnetic field was carefully made to determine the field fringing. Fig.2 shows the radial profile of the magnetic field while the magnet is energized with 100.00 amperes.

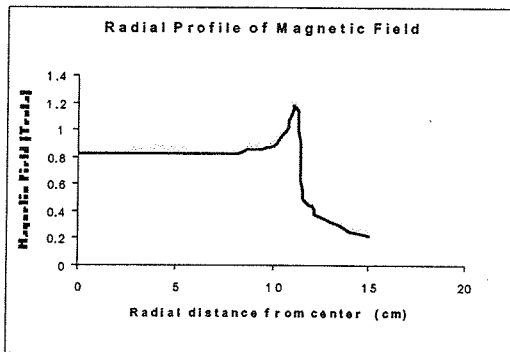


Fig2.Radial profile of magnetic field.

Uniformity of the magnetic field is extremely precise. The surfaces of the two poles are parallel with 0.001 inches. As will be seen later, the poles and yoke are slightly deflected due to the extreme pull of the electromagnetic force at high fields. No shimming of the magnetic field to increase the beam current has been attempted yet, however there are future plans to do so.

II. VACUUM CHAMBER. The vacuum chamber houses the DEE, the dummy DEE, the ion source, the ion collector, and ultimately hosts

the acceleration of ions. The chamber's construction is of a stainless steel wall, accessory ports, and flanges. The top and bottom lids of the chamber are of 0.25 inch aluminum. The lids make a vacuum tight seal to the circular stainless steel wall with the use of 451 Viton O-rings. The accessory ports were TIG welded and are terminated in either CF2.75 or CF1.33 metal gasket seal flanges. The vacuum port on the chamber is a standard KF25 Viton O-ring seal. The chamber has an inside diameter of 11.00 inches and a wall thickness of 0.750 inches. The outside height of the chamber measures 2.00 inches and the inside height measures 1.50 inches. The DEE is 1.00 inch thick allowing for 0.25 inches of clearance between the top and bottom of the lid. The DEE wall is 1/16 inch thick brass. The DEE and chamber are symmetrical about the chamber's median plane. The chamber's median plane is adjusted to be the same as the magnetic field's median plane. The DEE is supported by a 0.500 inch copper rod that is mounted to a CF2.75 flange. This whole assembly is then suspended from the chamber by a ceramic brake terminated with CF2.75 flanges at either end. This provides a substantial vacuum tight high voltage feed-through. The copper stem protrudes the vacuum flange by several inches allowing direct connection to the high voltage terminal in the RF matching cabinet, which is mounted just outside of the magnet coils. The Dummy DEE is mounted diametrically in the chamber making excellent electrical contact as it provides the aperture of the second accelerating electrode. The dummy DEE also provides a central mounting surface for the ion source. The chamber was assembled with three view ports, one ion vacuum gauge, one ion collector in the form of a faraday cup at the end of a radial linear positioner. In addition to the faraday collector, a phosphorescent screen also located at the end of a radial positioner. A capacitively coupled RF pickup probe also occupies an accessory port, this pickup resides behind the DEE.

III. VACUUM SYSTEM The vacuum system is a straight forward diffusion pump system that is backed by a direct drive mechanical pump. The Precision mechanical pump has an absolute pressure of 1E-4 Torr, and a pumping speed of 195 liters/minute. The diffusion pump is a Veeco 4 inch water cooled pump that uses Dow Corning 704 oil, with water cooled baffles, and a liquid nitrogen trap. The ultimate pressure of this four inch pump is 1E-8 Torr and has a

pumping speed of 425 liters/minute. Directly after the LN2 trap the plumbing steps down from a four inch flange to a two-inch KF40 Viton flange. A valve manifold and 18 inches of two-inch metal bellows connect the LN2 trap to the chamber. Only at the chamber does the vacuum line reduce to one-inch. After great care in assembling a clean and tight vacuum system the chamber can routinely be evacuated to 1E-5 Torr in approximately 30 minutes, and < 5E-6 Torr in less than 2 hours. The ion vacuum gauge on the chamber is the primary vacuum monitoring system, it also is a Veeco product, model RG-1002 Bayard-Alpart type gauge. Because it is mounted directly on a chamber accessory port, the gauge is in a significant magnetic field while the magnet is energized. Since the operation of the ion gauge utilizes low energy ion currents, even the slightest magnetic field will alter the ion current incident on the collector. This ion current change thereby guarantees erroneous pressure readings.

IV. RF OSCILLATOR. MOPA – Master Oscillator Power Amplifier ideology was decided upon as it is known to be the most stable as well as the simplest to invoke. The MOPA system oscillates at the driving frequency with great stability, even under glow discharge conditions. However, because the cyclotron tank circuit possess a high Q, very careful tuning becomes necessary when ensuring maximum power delivery. Other oscillator systems were considered, such as an SEO – Self Excited Oscillator, where active feed back from a pickup loop in the chamber allows for the natural frequency of the tank circuit to be sought out and oscillate automatically. Another advantage of SEO systems is their characteristic to have a very high efficiency. However, self excited systems are very complicated and require utmost care from an experienced radio engineer to prevent unwanted modes of oscillations, known as parasitic oscillations.

Initially a commercial RF generator was intended to be used as the primary RF power source. It is capable of supplying 2.5 kW to a 50Ω load. The generator operates at a fixed frequency of 13.56 MHz – a standard commercial processing frequency. Initial tuning and tank circuit preparations were conducted

with this generator. Thus, as mentioned earlier, adopting the frequency of 13.56 MHz as the operating frequency. However, it became evident that the RF power requirement was not so great, allowing a smaller RF source to be utilized.

An HP8165 digital programmable RF signal source was used to drive an ENI350L 100 watt solid state amplifier. This method was much more convenient as fine tuning was easily achieved at the signal source rather than by manually tuning the tank circuit. The smallest adjustment capable of the HP8165 is 10kHz, which proved to be sufficiently sensitive. The output of the ENI350L amplifier was then passed through a Bird wattmeter (model 4410) and on to the RF cabinet. The RF cabinet houses the impedance matching transformer which matches the RF power of the 50Ω line into a high impedance load – the DEE. The DEE being a very high impedance develops a high voltage alternating at 13.56 MHz, thus providing the high voltage for acceleration.

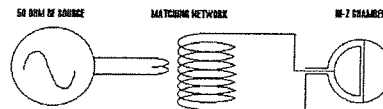


Fig.3 General cyclotron RF layout.

The transmatch may be recorded as the most home-brewed system of this cyclotron. It utilizes the lumped capacitance of the DEE, which is approximately 70pF, to create a tank circuit out of the chamber itself. Using the resonance equation for an inductor in parallel with a capacitor:

$$f_r = 1/2\pi\sqrt{LC}$$

L, the inductance, was chosen to bring the  $f_r$  to resonance at 13.56 MHz. Initially, coarse tuning was to create an 8 turn coil of length 5 inches, with a cross sectional area of 2.14 inches<sup>2</sup>, out of ¼-inch copper refrigeration tubing. The coil was then mounted

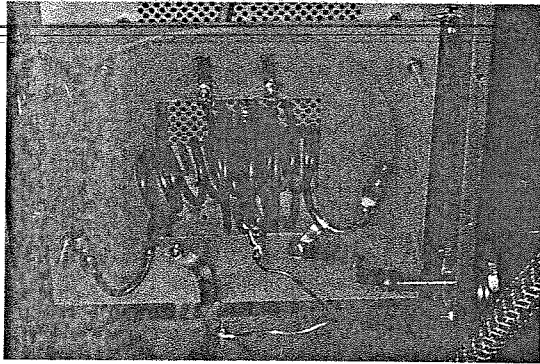


Plate.1 Transmatch in RF cabinet.

in an RF tight enclosure known as the RF cabinet. One end of the coil was connected to the protruding DEE stem, while the other end of the coil is connected to chamber ground. Another coil of copper tubing larger in cross sectional area, of only three turns, is mounted coaxially about the first coil. The outer coil constitutes the primary while the inner coil makes up the secondary of the transformer. Adjustable taps were then placed on the primary to locate the  $50\Omega$  loading point. Second order tuning was accomplished empirically. Either expanding or compressing the coil changed the inductance thereby altering  $f_r$ . Fine tuning was completed at the driving oscillator. Cooling became a necessity when the RF power began to heat the secondary coil such that thermal expansion changed the tank  $f_r$ . General Electric *Dielectrol* transformer oil is pumped through the  $\frac{1}{4}$  inch tubing of the secondary. The oil was then passed through a small heat exchanger that is cooled by flowing water. The oil is then returned to the pump reservoir of approximately two gallons volume. No effort was made to measure the cooling rate of the oil. There are future plans to remove the oil-water heat exchanger from the cooling circuit in order to perform calorimetry roughly estimating the tank circuit efficiency.

The Q of an oscillator follows several definitions which are interchangeable. Q is a unit less number describing the quality of an oscillator. Perhaps the best way to think of Q is the ratio of stored energy over lost energy per cycle:

$$Q = \Delta E_{\text{stored}} / \Delta E_{\text{lost}}$$

however there are several other definitions:

$$Q = \omega L / R = f_r / \Delta f$$

Q of the tank circuit expressed in terms of  $\omega L / R$  assumes no loading. Thereby  $\omega L / R$  is the theoretical maximum Q. For this cyclotron the non-loaded Q was about 1600. The measured Q

of the tank circuit is somewhat less due to loading, denoted as  $Q_L$ . Looking at the voltage developed on a capacitive pickup very loosely coupled to the DEE, a sweeping RF signal was injected into the transmatch. The voltage response was then plotted against frequency, shown in Fig.3. Using the Q formula,  $f_r / \Delta f$  the  $Q_L$  was measured.  $f_r$  was found to be 13.60 MHz. Because the response is measured in voltage rather than power,  $\Delta f$  is measured at 70.7% of the maximum height, which was found to be 90kHz. Thus the  $Q_L$  of the tank circuit was measured to be 150, a very reasonable  $Q_L$  for a tank circuit of this type.

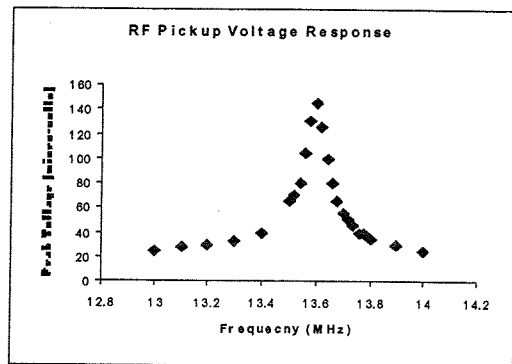


Fig.4 Q measurement of loaded tank circuit.

DEE voltage measurement and pickup calibration were completed with the use of the simple rectifier and voltage divider network illustrated in Fig.5. The high voltage capacitor, denoted as C1, was charged to the peak RF voltage through the rectifier and bled off by the high impedance resistor network. A DMM with a high input impedance was placed across R2 to

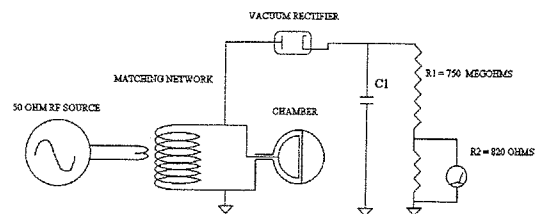


Fig.5 DEE voltage measurement circuit.

measure the developed voltage. The ratio of R2 to R1 is  $1:9.1E+5$ , thus the peak DEE voltage is:

$$V_{D\text{-peak}} = 9.1E+5 \times V_{R2}$$

Voltage measurements were taken as a function of incident RF power, as well as noting the induced peak voltage on the capacitive pickup to gain a simple DEE voltage reference. As expected, the peak DEE voltage rises as the square root of the applied RF power, Fig.6, and

the peak induced voltage is linearly proportional to the peak DEE voltage, Fig.7.

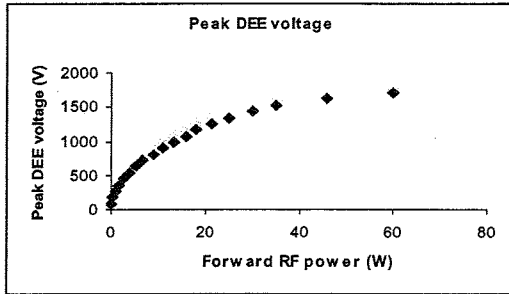


Fig.6 DEE voltage as a function of RF power.

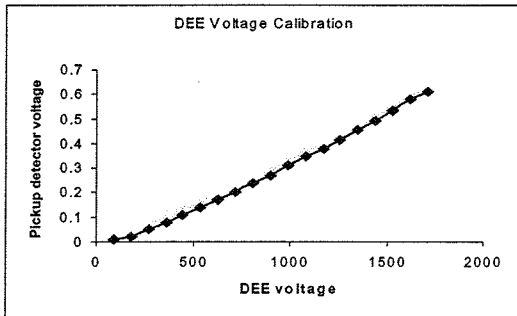


Fig.7 DEE capacitive pickup calibration.

When beginning RF testing it was thought that the chamber must be precisely centered in the magnet gap. To ensure centering, shims of equal thickness wedged the chamber in between the poles, snugly securing the chamber from top and bottom. When testing the RF system and the magnet together it was noted that at high magnetic fields the  $f_r$  moved down, as plotted in Fig.8. After an investigation it was decided that

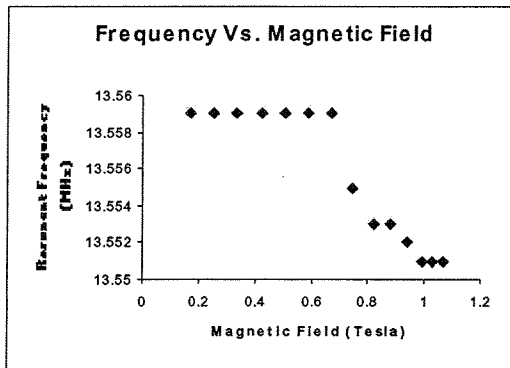


Fig.8  $f_r$  shift due to chamber compression.

the magnet poles must be attracting one another under the tremendous force, thereby squeezing the lids on the vacuum chamber. The inward movement of the lids would decrease the distance between the DEE and the lids creating an increase in chamber capacitance, thereby

bringing down  $f_r$ . The distance of movement was calculated from the change in frequency. Just using the approximation for a parallel plate capacitor the distance the gap decreased was on the order of 7 nanometers. The attractive force between the two poles was also estimated, at 1 Tesla the attractive force is approximately 16,000 N which the equivalent of placing a 3,500 pound mass on the top yoke. Under such forces it is reasonable to imagine deflection on the order of 70 Angstroms.

It is worth noting that even under maximum ion current conditions of 50 nanoamps no beam loading was noticed.

V. ION SOURCE. Since neutral hydrogen gas supplies the protons that will be accelerated, the hydrogen must undergo a process that will remove the electron and leave the positively charged proton behind. This is accomplished fairly easily by bombarding the hydrogen gas with low energy electrons. Located inside, close to the center of the top of the vacuum chamber the ion source is mounted on the face of the dummy DEE, see Plate 2. A W-Th-Ir filament is suspended between two electrical feed-throughs with spring loaded clamps at the tip. When approximately 7 amps flow through the filament it is heated to glow white hot. Since the filament is completely isolated from the chamber ground it can be negatively biased with respect to chamber ground causing thermionic emission to occur. A portion of the emitted electrons will pass vertically downward to the bottom of the chamber ionizing the hydrogen atoms present in their path. The electric fields of the ion source and accelerating RF sweep away the freed hydrogen electrons, leaving the massive protons behind. Further more, because of the very strong magnetic field parallel to the desired electron path, strong focusing occurs. Any electron that attempts to stray off of a vertical ascent or decent is immediately steered back towards the central axis of motion. Due to this corrective focusing, the electrons tend to oscillate back and forth in both X and Y while traveling downward in Z. Instead of following a linear path, the traversal then becomes a helical path with a very tight radius. The exposed filament is roughly 1 inch long, thereby producing a very thin sheet of electrons with a similar width of 1 inch. It was found that an optimum bias voltage of the filament was -320 Volts D.C.



Plate 2. Ion source filament arrangement

The thermionic emission rate is proportional to the heating of the filament. The heating of the filament is proportional to the square of the

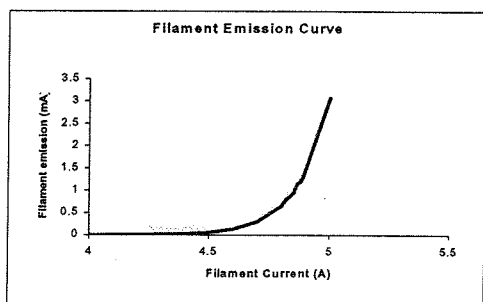


Fig.9 Emission of test filament, bias -300VDC

applied current. Fig.9 shows the exponential emission of electrons in a test of the W-Th-Ir material. Hence slight changes in the filament current can produce great changes in thermionic emission. Ultimately changing the number of thermionic electrons available to ionize the hydrogen. In this way the cyclotron proton beam current can be controlled. As of yet the limiting factor in the maximum achievable beam current at the periphery is due to filament heating limitations.

Hydrogen gas is emitted to the chamber via a calibrated leak. The leak is backed by a high pressure regulator that takes the hydrogen from a lecture bottle at a few thousand PSI and brings it down to approximately 10 PSI. The pressure setting is empirically controlled by monitoring the vacuum ion gauge with the magnetic field off. Because the vacuum system is continually pumping on the chamber a minute flow of hydrogen occurs with the chamber pressure leveled off at some equilibrium.

For pressures greater than  $5E-5$  Torr, and filament emission currents greater than 1 mA, a dramatic cathode ray appears. Plate 3 was taken through the view-port that looks down the accelerating gap. Electrons travel down from the filament along the magnetic field lines to the bottom of the chamber.

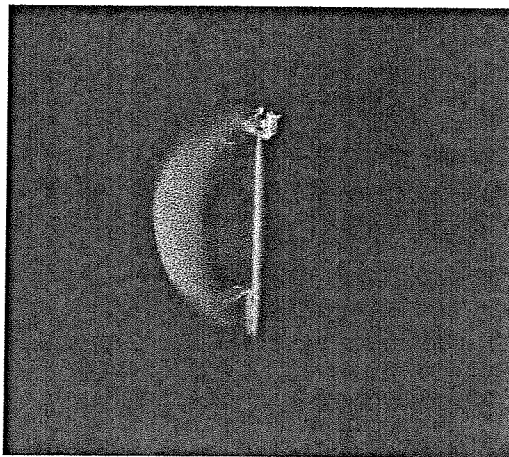


Plate 3. Ion Source Electron Beam.

It was found that the optimum hydrogen pressure was  $5.5E-5$  Torr. Pressures higher would decrease the collected beam due to the protons decreased mean free path, while pressures lower than optimum decreased the available hydrogen of which to create ions from.

VI. ION COLLECTOR. A simple faraday collector was incorporated to initially detect the accelerated ions. The principle of operation is simple: as a high energy proton hits a brass target it gives up its energy in the form a X-rays and thermal heating. The proton lodges itself into the brass, thereby implanting positive charge. If available the proton will collect an electron and neutralize again. If the brass target is connected to a source of electrons, such as ground, it is possible to count the number of incident protons by measuring the electron current that arises. An electrometer is placed in between the collector and ground making it possible to resolve picoamps of electron current. A consideration in beam current measurements is the creation of secondary electrons at the target from the incident high energy protons. 'Removal' of negative charge looks the same as addition of positive charge, potentially producing erroneously high current measurements. A small positive bias can be placed on the collector to suppress secondary electrons, but care must be

taken not to deflect incident protons by too high of a positive bias.

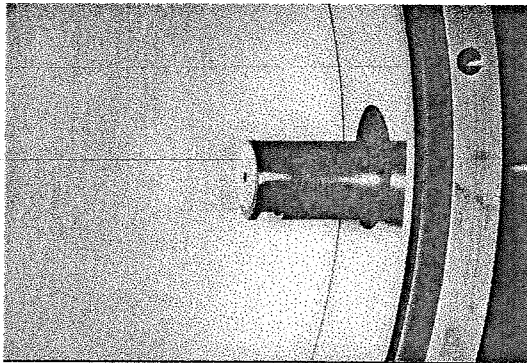


Plate 4. Ion Collector – at minimal insertion

This faraday collector was constructed from a 3/8 inch brass slug and is suspended as well as isolated in a coaxial arrangement by a Teflon spacer inside a 1/2 inch hollow copper cylinder. The copper cylinder forms an RF shielded housing for the brass slug. The copper cylinder has a 0.185 inch slit diametrically traversing one half of the hollow portion near the tip. This slit exposes the brass slug centered inside and is positioned such that it is only exposed to positively accelerated ions, while any negative ions hit the grounded RF housing. The current signal leaves the faraday collector by a short length of RG-174 coaxial wire. The RG-174 then connects to a coaxial vacuum feed through. Outside of the chamber a 15 foot length of RG-174 completes the connection to a Keithly 610CR electrometer. The recorder output of the 610CR was measured by a five digit Keithly DVM whose data is read out via HPIB. It was noted with a bias supply inserted in the electrometer line that there were minimal secondary electrons escaping.

The faraday collector assembly is mounted on a vacuum tight linear motion feed through. It is mounted such that the collector can be inserted radially with a two inch travel, effectively determining the maximum ion radius. The minimum measurable ion radius, maximum insertion of the collector is 2.50 inches while the maximum ion radius, minimum collector insertion is 4.50 inches. A plot of beam current against radius, Fig.10, shows that the beam current linearly drops off as the radius grows.

The second ion collector, in the form of a phosphorescent screen also located at the end of a linear positioner was inserted into the beam

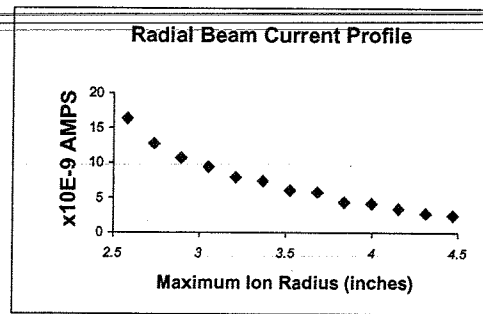


Fig.10 Radial Beam Current Profile.

region to locate the beam. Indeed, brilliant illumination occurred where the beam was incident. However, after a short period of ion bombardment the luminescence ceased. This is due to the charging of the screen, the strong electric field that developed deflected the incident proton beam off target. The screen charging issue was resolved by sputtering approximately 50 Angstroms of gold over all of it's surfaces and ensuring a connection to ground. Such a thin layer of metal is almost completely transparent yet conductive. After metallization the beam indeed re-appeared and remained on the screen without any deflection, Plate5.

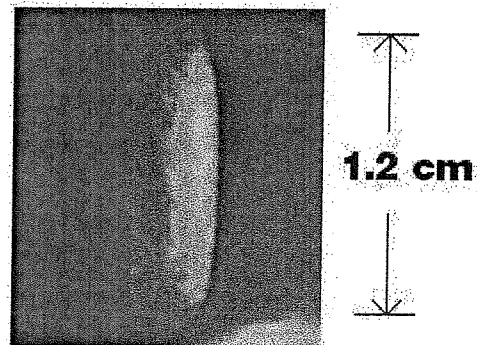


Plate5. Beam visual on flag.

VII. DAQ / CONTROL Although considered obsolete in this day, the HP85 proved to be an extremely versatile piece of test equipment. It's ability to control any HPIB ready unit has made possible a flexible data control and acquisition system. The simple HP Basic language allowed even the most novice programmer to exercise complete equipment control. Although the processor is slow, speed was not an issue as the magnetic field needed to be ramped even slower. Future needs that may arise from active feedback certainly would require a faster computer. A minimum of data manipulation was completed by the HP85, all data that was collected was

immediately transferred to a PC via an RS232 link. The PC terminal program wrote all data to disk leaving analysis to be completed off-line.

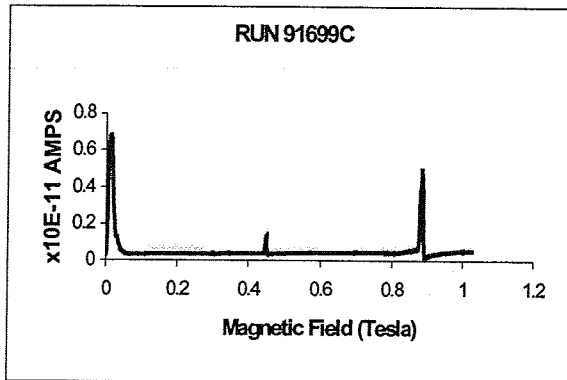


Fig.11 Early detection of beam.

VIII DATA Typically, a run consists of slowly ramping the magnetic field while monitoring the beam current for a given set of parameters. The second successful resonance run plot, 91699C, is shown in Fig.11. As expected a strong proton current developed at the magnetic field corresponding to the  $f$ . In run 91699C the resonant frequency was tuned to 13.590 MHz. Other parameters for run 91699C are listed below:

$f$	13.590 MHz
Forward RF Power	16 Watts
Theoretical B-field	0.889 Tesla
H <sub>2</sub> Pressure in tank	5.1E-5 Torr
Filament Current	5.75 Amps
Filament Voltage	5.0 Volts
Filament Bias	-320 Volts
Filament Emission	21.0 $\mu$ Amps
Max. Ion Radius	7.0 cm
Max. Ion Energy	184 keV

The measured ion peak at 0.885 Tesla tightly corresponded with the theoretical value to 0.6%. The development of the 0.885 peak was rewarding confirmation that this nine-inch cyclotron work as designed. However an unexpected peak at 0.449 Tesla developed. Since hydrogen, being the fundamental element, has a Q/m ratio of  $1e^+/1amu$  it was hard to imagine what ion was being accelerated, for it must have fractional mass or excessive charge if it were arising from the fixed  $f$ . Several runs were taken with increased ion current sensitivity, in order to determine reproducibility as well as stability, Fig.12. After an investigation into the matter, it was determined that indeed singly charged protons were being accelerated.

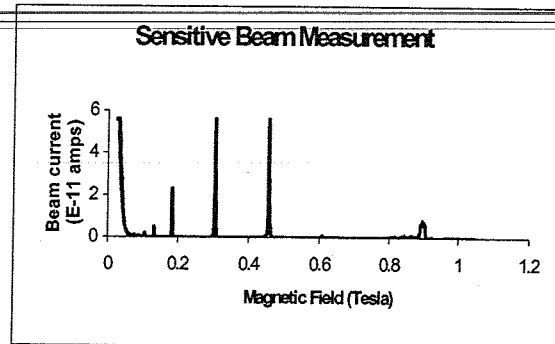


Fig.12 Sensitive beam measurements.

Although, not obvious at first, the RF frequencies required for acceleration of the ions at the low magnetic fields, developed from excitation of higher frequency modes of oscillation in the tank circuit. These are known as harmonics of the fundamental  $f$ . Even at that, the harmonic frequencies that developed would require higher magnetic fields, not lower. At this point some detailed thought of the accelerating electric field is required.

As shown earlier, the RF period needs to equal the angular frequency of the circulating ion, such that the electric field always points in the same direction as the ion's velocity when entering the accelerating gap. If the applied frequency were double that of the fundamental, on it's second crossing of the gap the ion would receive a deceleration, thus gaining zero net acceleration. However, if the RF frequency were triple that of the fundamental it is seen that the electric field direction is again in sync with ion's travel. This effect holds true for any odd multiple of the fundamental cyclotron frequency. Acceleration measured at the low magnetic fields were a result of the harmonic frequencies being odd multiples of the ion's required fundamental cyclotron frequency. These harmonics were confirmed and measured with the use of a network analyzer. Because of the shorter period, the duration of the electric field in the appropriate direction is also less, causing increased magnetic field precision requirements, hence the sharpening of the beam current peak seen in Fig.12. In order to maximize the RF systems efficiency these harmonics should be suppressed. Future RF work will attempt this feat.

IX. DISCUSSION. Sufficient data has been taken with this feasibility-study cyclotron to warrant progression to a twelve inch magnet. It is reasonable to expect one million volt protons



with a magnetic field of 1.2 Tesla, and an  $f$  of 18 MHz. Such a magnet system is currently being obtained.

Had more time been spent on improving the ion source, undoubtedly 1  $\mu$ A of accelerated beam could have been achieved. However, this study will be reserved for the twelve inch magnet. Sources such as capillary discharge tubes will be implemented.

The larger fixed frequency RF source is still available to our lab, however it must undergo a series of modifications to operate in the desired frequency range of 18 MHz. Other options are also being explored, such as the use of a large tunable metal-ceramic sealed vacuum tube power amplifier driven by the ENI350L. The use of a solid state amplifier is precluded once power requirements exceed 500 Watts.

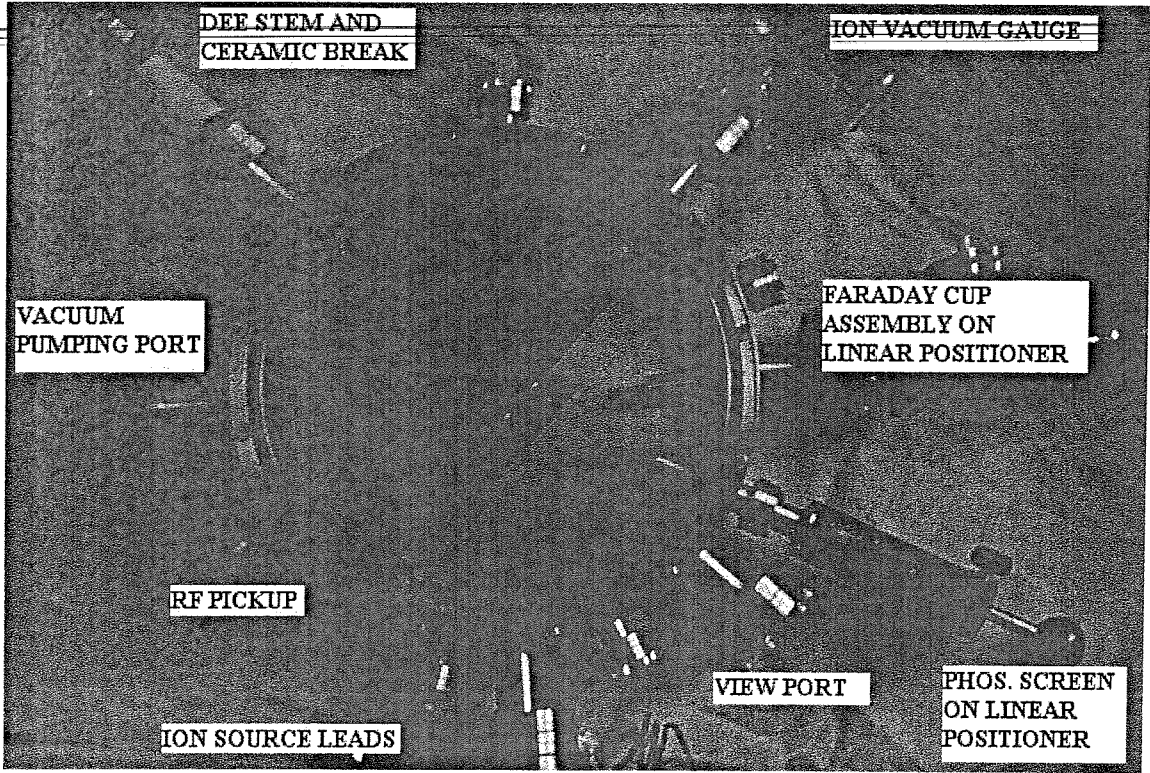
Finally, after the twelve inch system has proved operable, a tangential accessory vacuum port will be added with the intention to extract the proton beam. This final addition will complete the readiness of the twelve inch cyclotron for research use.

X. ACKNOWLEDGEMENTS Many thanks goes to the generosity, ingenuity, and patience of all the following: K. Carlson, Dr. P. Colstock, Prof. M. Croft, J. Doroshenko, V. Eng, F. Ernst, L. F. Ernst, Jr., L. F. Ernst, Sr., M. M. Ernst, R. Frisch, Prof. M. Gershenson, E. Halkiadakis, S. C. Hanebuth, K. Hansen, R. P. Hansen, J. F. Koeth, W. J. Koeth, R. B. Krawchuck, J. Krutzler, Dr. M. Kuchnier, J. Kuhl, Dr. M. Molnar, V. Myrnyj, Dr. R. Pfeffer, Prof. J. Pifer, W. Schneider, L. Wahl.

#### XI. REFERENCES

- The Production of High Speed Ion Without the Use of High Voltages, E. O. Lawrence and M. S. Livingston, 1932
- Particle Accelerators, M. S. Livingston, 1962
- El Cerrito Cyclotron, Physics Today, 1:10, 1948
- The Development of High Energy Accelerators, M. S. Livingston, 1966
- Particle Acceleration, J. Rosenblatt, 1968
- Lawrence and Oppenheimer, Huel Pharr Davis, 1968
- The Radio Amateurs Handbook, ARRL
- Engineering Electromagnetics, Hayt, 5<sup>th</sup> Ed., 1989
- Microwave Tubes, A. S. Gilmore, Jr., 1986

- An Introduction to the Physics of High Energy Particle Accelerators, D. A. Edwards and M. J. Syphers
- Particle Accelerators and Their Uses – Part 1, Waldemar Scharf, 1986
- Inductance Calculations, F. W. Grover, 1946
- Lawrence and His Laboratory, J. L. Heilbron and R. W. Seidel, 1989
- Radio Engineering, Terman, 3<sup>rd</sup> Ed., 1947
- Introductory Nuclear Physics, K. S. Krane, 1988
- A User's Guide to Vacuum Technology, J. F. O'Hanlon, 1980
- Particle Accelerator Physics 1, Weidemann, 2<sup>nd</sup> Ed., 1999
- Electromagnetics, J. D. Kraus, 4<sup>th</sup> Ed. 1992



---

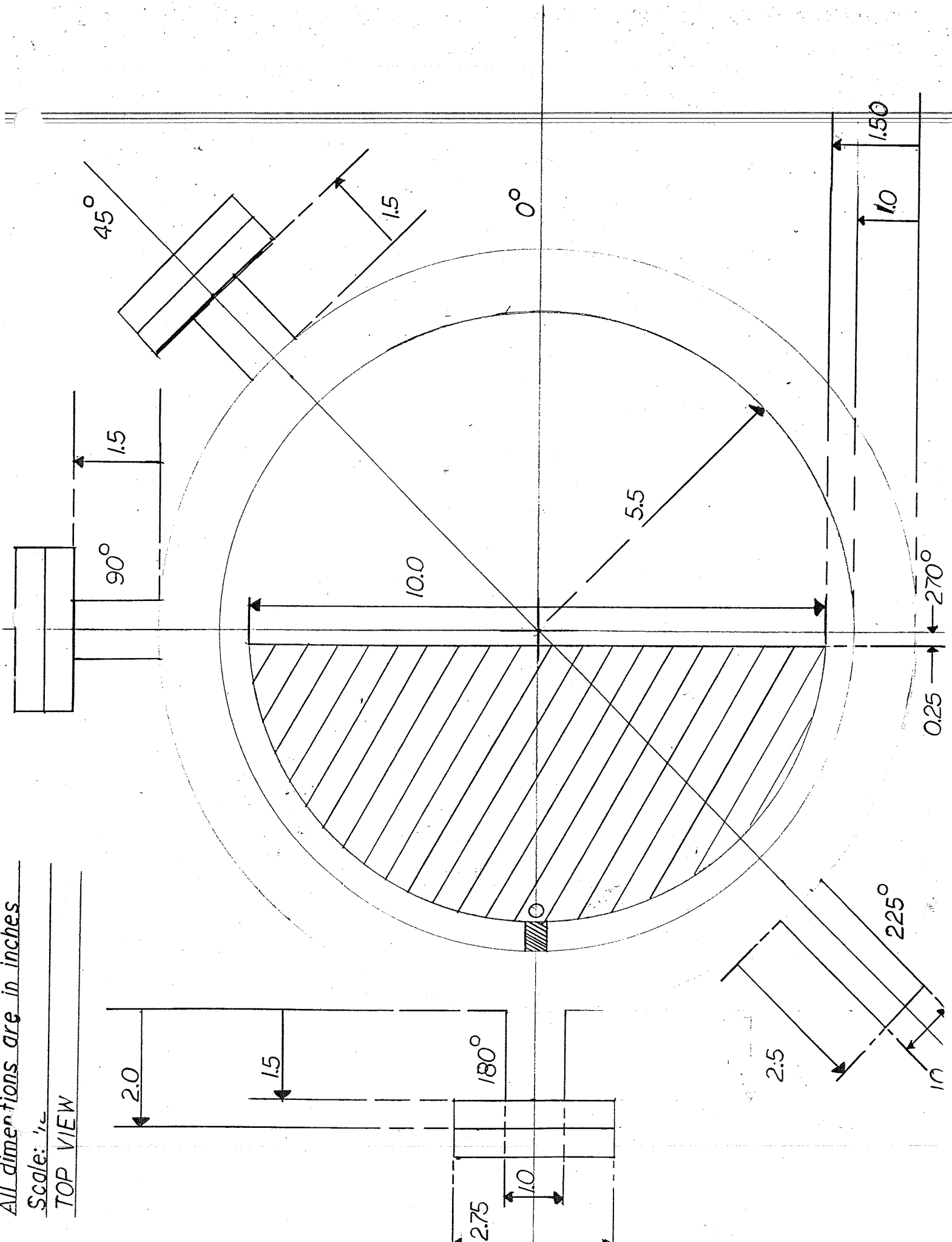
# **APPENDIX 1**

Detailed drawings of Cyclotron Chamber and Dees

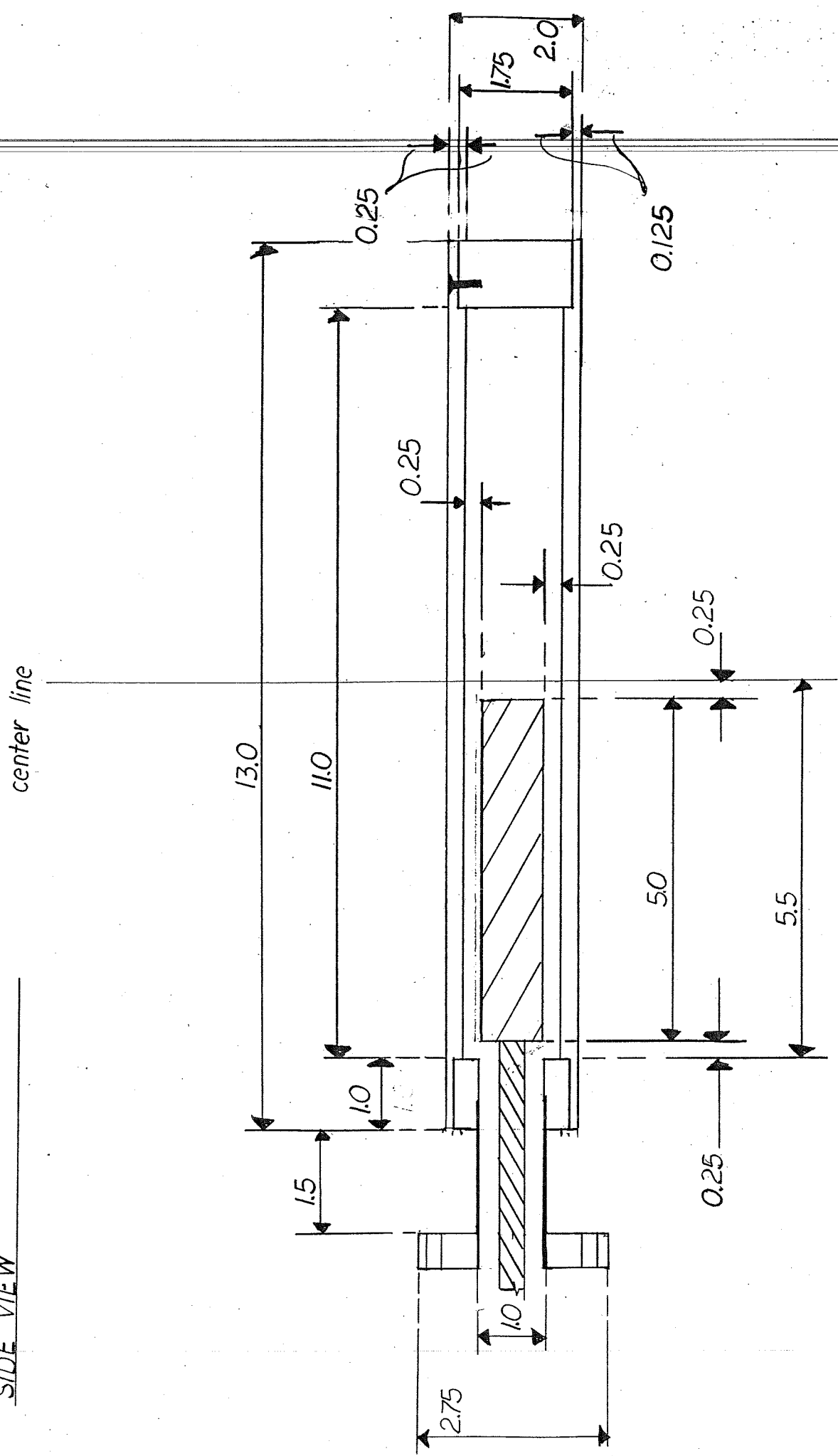
All dimensions are in inches

Scale: 1/4"

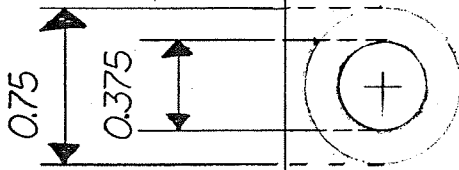
TOP VIEW



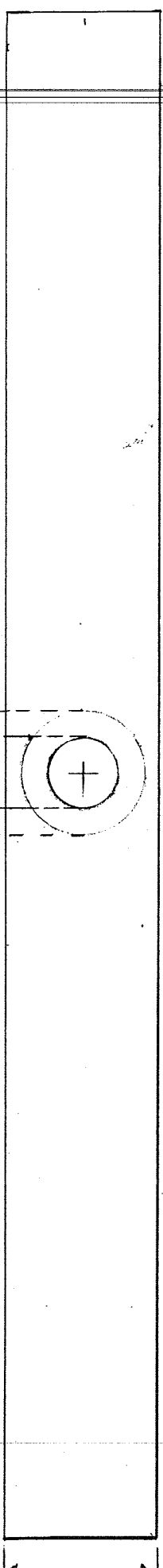
All dimensions are in inches  
 Scale: 1/2  
 SIDE VIEW



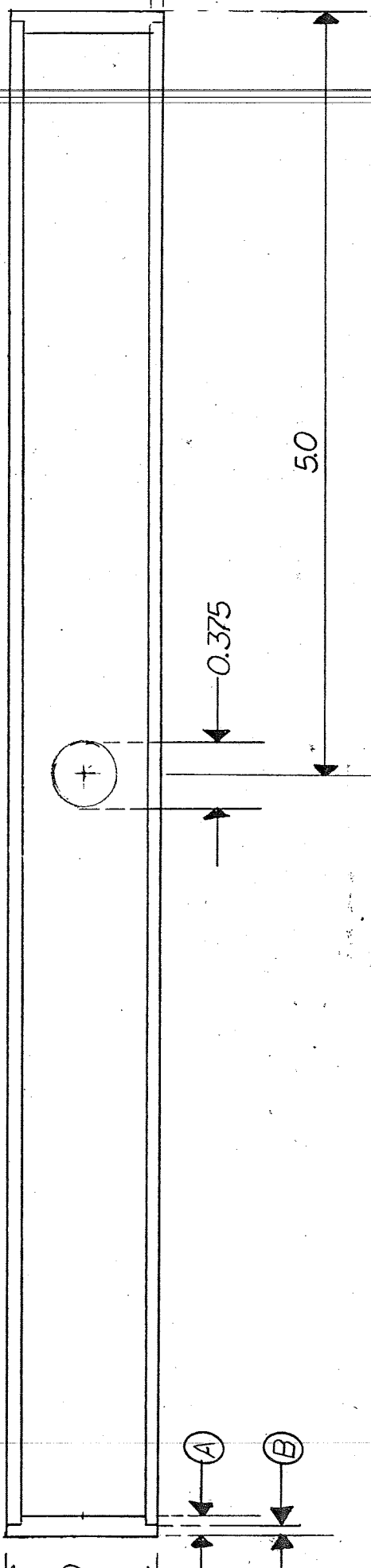
BACK VIEW



ACTUAL SIZE



10.0



5.0

0.375

A

B

C

OPEN FACE VIEW

NOTE: DIMENSIONS A, B & C ARE TO BE DETERMINED BY SHOP.

ASSC. PORT 1

ASSC. PORT 2

0.5

DEE MIRRORED FACE

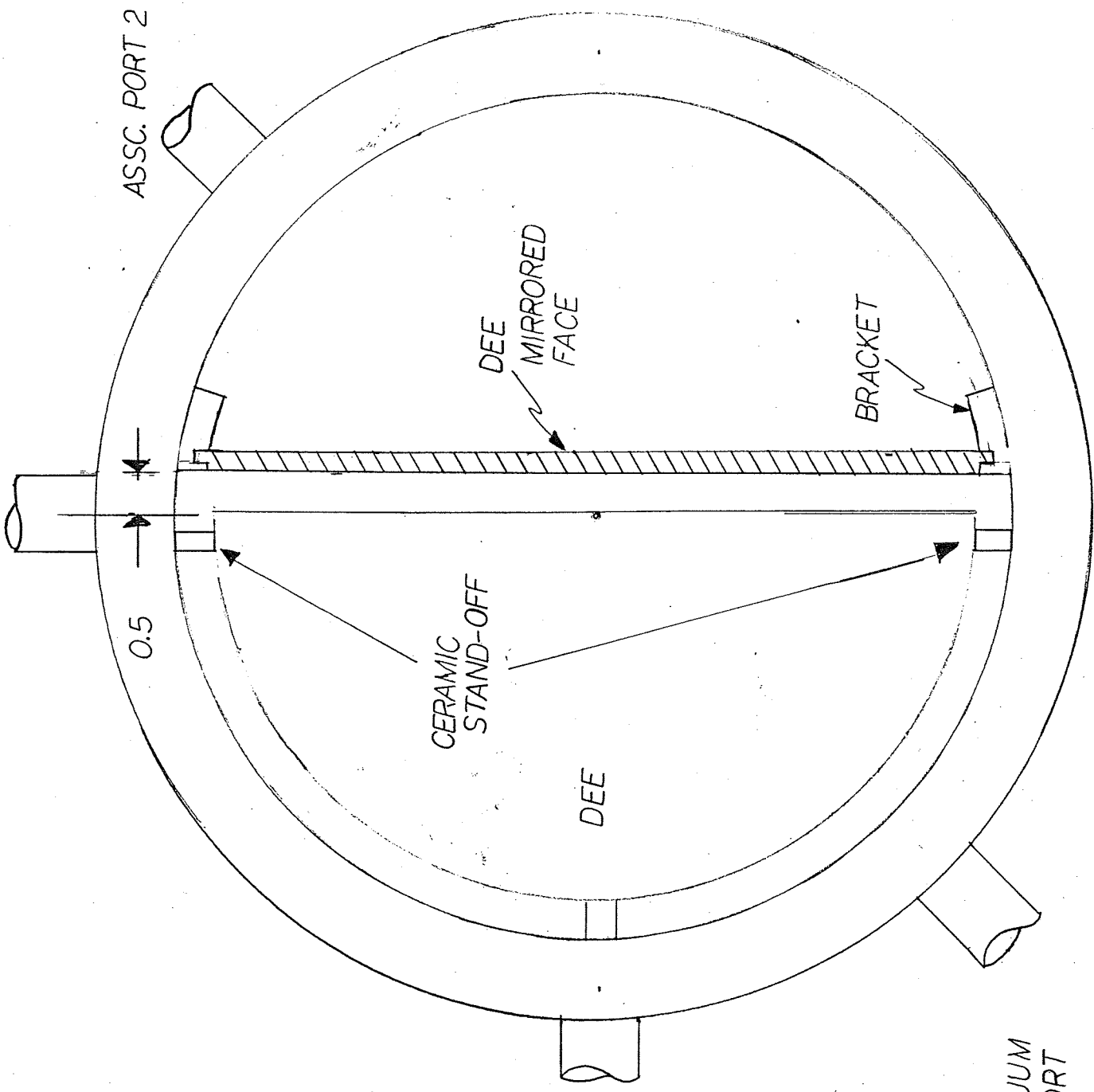
BRACKET

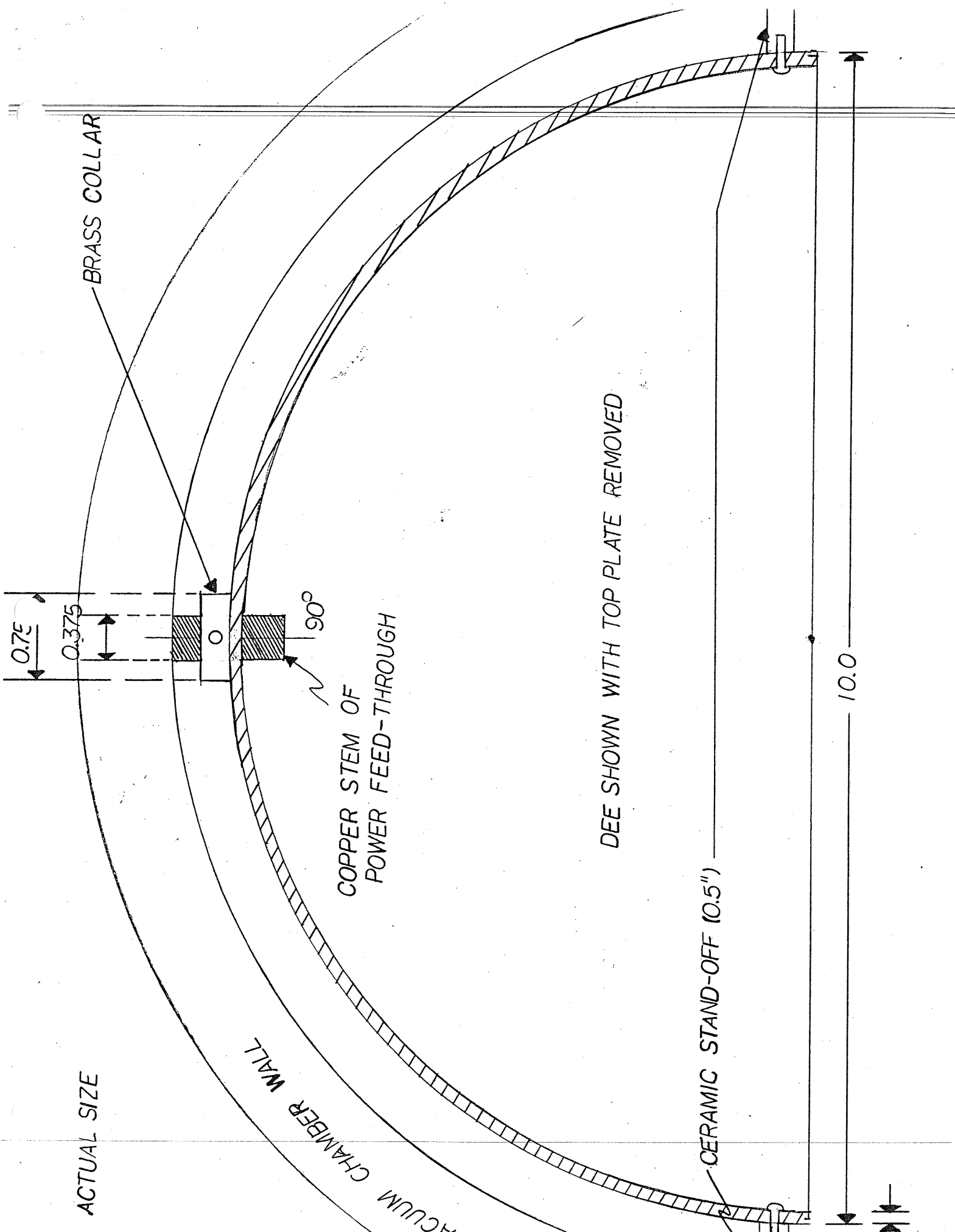
CERAMIC STAND-OFF

DEE

POWER FEED-THROUGH

VACUUM PORT







ACTUAL SIZE

SIDE VIEW

